Published by :
http://www.ijert.org

International Journal of Engineering Research & Technology (IJERT)
ISSN: 2278-0181
Vol. 7 Issue 02, February-2018

Observation of Turbulent Velocity Wind Profile Low Level Jet

Shweta Thakur [1] & S. K. Jain [2]
[1-] Barkatullah University Bhopal 462026
[2-] Institute for Excellence in Higher Education, Bhopal 462016

Abstract: **Distributions of the shear exponent (α) computed fig. 5.6 by lidar horizontal velocities measured at 115, 200, 250 m and reference velocity at 20 m for the entire period of HRDL observations have been made. In most cases α > 0.20, with a dominant mode of 0.30-0.36. μ is turbulence variable in the stable surface layer σ/U near to the surface. This is despite the fact the variance itself shows the greatest uncertainty near the surface. Estimates of U and σ from several studies, ratio of σ/U from individual profiles have an average range is 0.20. The studies of night indicate that composite value is 0.20.**

Key Words: Low level Jet, Turbulent velocity and wind Profile.

1. INTRODUCTION:

Turbulence or flow could be a flow regime in fluid dynamics characterized by chaotic changes in pressure and flow speed. It is in distinction to a streamline flow or laminar flow regime that happens once a fluid flows in parallel layers with no disruption between those layers. LLJ have been shown to occur frequently in many parts of the world including the peninsular and western Indian region using radiosonde data. The data of radiosonde observations in Indian region are taken at 0000 and 1200 hrs GMT. These low level wind maxima and found to be associated with the development and evolution of deep convection. Since deep convection activity produces a significant amount of middle/upper level cloudiness. The relation between LLJ and convective activity indicates that LLJ are important contributors to regional as well as global climate.

LLJ appearance around 850-500 hPa during the Asian summer monsoon in the peninsular and western region of India is closely associated with the active period monsoon. It has been noted of south west monsoon over the west coast part of India upper and middle winds of jet streams at low level.

Study of turbulence profile were measures have typically found maximum of turbulence quality at the surface decreasing to minimum monotonically to a minimum at the top of the stable boundary layer traditionally boundary layer structure. Caughey et al. (1979) found this structure using data obtained between dusk and midnight from a 32 m tower and a tethered balloon system during the 1979. Smedman et al. 1993, 1995, 1997, 2004; Tjernstrom and smedman 1993 studies of turbulence Mahrt et al (1979), the connection between LLJ and turbulent mixing was further explored in a comprehensive series of measurement projects over the Baltic sea using instrumented towers, special rawinsonde and pibal ascents and aircraft slant path profile.

Low level jet plays an important role in the generation of shear in the layer between the jet maximum and the earth surface. Mahart et al. 1979; Lenschow et al; 1988; smedman et al. 1993, 1995, 1997: Tjernstrom and smedman 1993; Mahrt 1993; Mahrt and vickers 2002; Banta et al. 2002, 2003; This shear often an important source of turbulence and fluxes in the nighttime boundary layer. Accurate determination of turbulent fluxes is important for transport and diffusion application, including air quality and emergency response and for improvements in the representation of these processes in numerical weather prediction (NWP) models (Mahrt 1998; Beyrich 1994; Banta et al. 1998, 2005; Andreas et al. 2000). Two type of vertical turbulence structure have been identified one the traditional boundary layer in which turbulence is generated at the surface and transported upward in contrast to the second type where turbulence id transported downward from a primary source in boundary layer. A number of studies have presented measurements spherical condition as well as profile for stable cases where no level wind maximum could be defined. Lenschow et al. 1988; Smedman et al. 1993, 1995; Tjernstrom and Smedman 1993 studies of low level jet structure over the great plains and the gold Balstic sea using aircraft slant profiles, turbulence kinetic energy was found to decrease with height from a maximum value at the surface to a minimum at the top of the stable boundary layer, indicating traditional rather than upside down structure according to the criteria described in Mahrt and vickers (2002).

Joseph and Raman reported the existence of low level westerly jet over peninsular India during South-west monsoon and showed that the LLJ are seen intermittently with varying frequency and intensity in the period June-September all the way of middle latitude and that the highest frequency occurrence appears in the month of July and the maximum wind speed are typically observed at heights below 2.4 Km. It is known that the strength of low level monsoon winds over western India is directly related to the rainfall. In his study result concluded that the LLJ observed in peninsular / western India in July are part of a branch of Somali Jet (high speed wind flow from Kenya to eastern Ethiopia and Somalia). In the month of July and August strong westerly winds are common in the western and peninsular India and are concentrated in the height range of 1.5-3 Km. The strong westerly LLJ around 2 km passing to

International Journal of Engineering Research & Technology (IJERT)
ISSN: 2278-0181
Vol. 7 Issue 02, February-2018

mid latitude has been cited as one of the necessary criteria. LLJ defined under the following condition (Joseph and Raman):

1. The wind speed maximum is below 6 Km.
2. Wind direction substantially unaltered throughout the height range ~ 40°.
3. Wind direction should be sharply decreases on either of wind maximum though it should be sharper on the lower side.

It is work noticed that the monsoon (westerly/south westerly) LLJ is expected to attain a maximum wind speed of typically around 15 ms^{-1}. In this region friction decoupling leading to LLJ acceleration Blackadar (1957) mechanism was accomplished by spatial advection of column of temporal nocturnal surface cooling (Hogstrom and Smedman 1984). Many profiles of mean and turbulence quantites presented or analyze reveal a prevalence of traditional structure. Comparison of turbulence measurements for profiles with and without LLJ structure show distinct difference, including a much more distinct spectral gap for cases with LLJ. The suppression of low frequency spectral energy in the gap region was attributed to the inhibition of larger scale fluctuation such as gravity waves and two-dimensional inactive turbulence by the presence of the jet (Smedman et al. 1995, 1997). Turbulence profile observations in the weakly stable boundary layer have thus shown traditional boundary layer structure. Analytical models of turbulence profiles for the stationary, horizontally homogeneous SBL with continuous turbulence also show this structure. Nieuwstadt (1984) derived a paramter from equation of motion Richardson number and flux Richardson number (R_i = R_{if} = 0.2). Result was a traditional boundary layer structure, with maximum fluxes and variances at the surface decreasing with height to 0 at z/h = 1, where h is SBL depth. Model kinematic stress is decreased as the 3/2 power of height$\frac{\tau}{u2} = \left(1 - \frac{z}{h}\right) 3/2$. Lenschow et al. (1998) derived a similar model of the SBL but with a thermodynamic energy equation that was expandedto include a radiative cooling profile as result momemtum flux decresed 1.75 power of z and the heat fluz $z^{3/2}$. Sorbjan (1988) recommended 1.5 and 2.0 for the values of these exponents, respectively. Numerical large eddy simulation runs also produce this behavior with a maximum at or just above the surface (Kosovic and curry 2000; saiki et al. 2000 and Derbyshire 1990). Smedman et al. (1995) interpreted their finding as showing that turbulence produced in the shear layer below Z_x is transported downward by the pressure transport term to layer near to surface. Mahrt and Vickers (2002) refined the definition of this type of boundary layer as one in which TKE (or σ^2_w) increase with height, turbulent fluxes increased with height and turbulent transport or velocity varies (σ^3_w) is negative.

2 HIGH RESOLUTION DOPPLAR LIDAR:

The High Resolution physicist measuring instrument (HRDL) may be a system capable of measure and mapping part velocities and scatter with the high preciseness and rate necessary for physical phenomenon studies necessary to understanding weather, climate and air quality. Analysis applications include:

- High spatial temporal and rate resolution wind profiles
- Boundary layer turbulence and entrainment zone studies
- Flux measurements
- LES model low-level formatting and validation
- Temporally and spatially averaged measurements of divergence
- Multi-platform operations: land, ocean and air

2.1 Basic Parameters Measured

- Range resolved line-of-sight velocity profiles
- Range resolved backscatter intensity

Wavelength, Pulse energy	2.0218 µm, 1.5 mJ
Laser	Tm:Lu,YAG diode-pumped, injection-seeded laser
Maximum and Minimum range	2 - 9 km and 0.2 km (typically 3 km)
Velocity Precision	5 cm/s
Time and Range Resolution	0.02 s (for 10 pulse average) and 30 m
Scan and Frequency stability	Upper hemisphere and 0.2 MHz
Pulse rate and Pulse energy	200 Hz and 1.5 mJ

Table 1 Technical specification of HRDL

3 SODAR:

SODAR (Sonic Detection and Ranging), additionally written as sodar, could be a earth science instrument used as a wind profiler to live the scattering of sound waves by region turbulence. SODAR systems area unit} accustomed measure wind speed at numerous heights on top of the bottom, are physics structure of the lower layer of the atmosphere. Sodar systems are like measuring device (radio detection and ranging) and measuring system (light radar) systems except that sound waves instead of radio or light-weight waves are used for detection. Alternative names used for sodar systems embody device, echosounder and acoustic measuring device. Traditionally employed in atmospherically analysis, sodars ar currently being applied as another to ancient wind watching for the event of alternative energy comes. Sodars used for alternative energy

International Journal of Engineering Research & Technology (IJERT)
ISSN: 2278-0181
Vol. 7 Issue 02, February-2018

applications are generally centered on a measurement range from 50m to 200m on top of ground level, similar to the dimensions of contemporary wind turbines.

4 DATA:

To investigate thunderstorm turbulence flow of wind. During the event of storms data were recorded by National Oceanic and Atmospheric Administration (NOAA) Center. These datasets has been taken from Earth System Research Laboratories (Global Monitoring Division) of NOAA center from www.ersl.noaa.gov for American Samoa Observatory and www.ersl.noaa.gov/csd/projects/lamar/wind.html. Satellite thermal based images have been taken High Resolution Doppler LIDAR (HDRL) and SODAR.

5 METHEDOLOGY:

Poulos et al. (2002) the development of surface airborne and remote sensing instrumentation to study the nocturnal stable boundary layer discussed. One of the instrument deployed was the High resolution Doppler Lidar (HRDL) described by Grund et al. (2001) with modification detailed in wulfmeyer et al. (2000). HRDL receive and emit backscattering from infrared radiation light pulses which are used to probe the aerosol backscatter and Doppler velocity structure of the atmosphere. Banta et al. 2002 and 2003 Range of HRDL during was ~2km spatial resolution of the velocity measurements was 30 m range and the velocity precision was ~10 cm s^{-1}. Kelley et al. (2004) this data have been used studies of LLJ structure atmospheric wave. LLJ formation during night is very important for wind energy operations. LLJ provide enhanced wind speeds to drive the turbine, one issue failure of turbine hardware as result of significant nocturnal bursts of turbulence. Banta et al. (2006) LLJ 03 instrumentation included a 120 m tower instrumented at four levels and three components Doppler SODAR operated. The tower instruments three axis sonic anemometers mounted at height of 54, 67, 85 and 116 m to provide three component winds and temperature data at the sampling rate of 20 Hz. Night time HRDL data collected from 1000-1200 UTC. Banta et al. (2003) Bulk Richardson numbers were calculated from data as described. The gradient bulk Ri calculation

$$\mathrm{Ri} = \frac{g\Delta\theta/\Delta z}{\theta(\Delta U/\Delta Z)2}$$

Ri values calculated to be constant height and equal to the bulk values a result of the roughly linear profile of U and θ between the top of the surface layer and Zx. (Banta et al. 2003; Poulos et al. 2002).

The onset of turbulence may be foretold by a dimensionless constant known as the Sir Joshua Reynolds range that calculates the balance between mechanical energy and viscous damping in a very fluid flow.

$$Re = UL/v$$

U is the characteristic velocity scale; L is the characteristic length scale and v is kinematic coefficient of viscosity of the fluid. For example in the flow of water in a circular pipe, the diameter of the pipe and the velocity of water at the center of the pipe will serve as the characteristic length and velocity. The transition to turbulence typically occurred in the Reynolds experiments when the Reynolds number exceeded the value of the ~2300 although it is possible to delay the onset of the transition to turbulence by ensuring that the roughness associated with the surface of the circular pipe is kept as minimum. Banta et al (2006) found Lidar variance overestimated tower measured stream wise variances or TKE.

5.1 Equations of mean motion in turbulent flow:

Chandrasekhar (2013) observation of velocity components with time reveal that the turbulent flows have underlying the irregular fluctuations a component which is rapidly varing with time.

$$\mu = 1/\mathrm{T}\int_{t-T/2}^{t+T/2} udt$$

T is averaging time T is chosen to be such that it is long enough so that the underlying widely fluctuations are smoothed out and the slowly varying component is observed. μ is x component
of velocity. In each of atmosphere studies turbulent velocities were scaled by surface layer friction velocity μ_* and height were perpendicular using the boundary layer depth h. The defination of h varied from ones based on mean quantities (Tjernstrom and Smedman 1993) to ones based on the decrease with height of turbulence quantities. For example caughey et al. 1979 height were heat flux decreased to 5% of its surface value. Similary TKE decreased by 95% (Lenschow et al. 1998; Sorbjan 1988).Nieuwstadt 1984; Beyrich 1994 gives SODAR back scatter decreases abruptly. Height of LLJ speed maximum abbreviated here Z_x represented an upper bound to the vertical extent of turbulent transport because peal value of Reynolds stability (Mahrt et al. 1979). They show that the depth of the nocturnal temperature inversion Z_I increase in time thrugh the night to become routinely larger than Z_x. Banta et al.(2006) found Z_x to be the height of first wind speed maximum above the surface representing the depth of the surface based shear layer.

Turbulence K.E. (TKE) is that the mean K.E. per unit mass related to eddies in flow. Physically, the turbulence K.E. is characterized by measured root-mean-square (RMS) rate fluctuations. Profile terms of the TKE budget were evaluated to determine the process controlling the structure of the vertical turbulence profile. The profile was maintained by a near balane between shear production and dissipation throughout the depth of the SBL (Lenschow et al. 1988; Sorbjan 1988; Tjernstrom and Smedman 1993; Smedman 1995) and supression of TKE by stratification was small but non zero.

6 RESULTS:

Composite profiles for the night fig. 2 measure below, showing wind speed U_h, stream wise variance σ_U, and turbulence intensity TI (σ_U/U_h), show a powerful turbulence below the peak of the LLJ most. The mean wind

International Journal of Engineering Research & Technology (IJERT)
ISSN: 2278-0181
Vol. 7 Issue 02, February-2018

profile with relatively small scatter. z/z_c profile is the subject layer has a slight convex curvature and the profile linear to slightly concave curvature. σ^2 are largest near to surface, σ^2 and σ profile exhibit a minimum at LLJ height. All heights square measure normalized by the peak of the LLJ maxima (Zc). Turbulence intensity as shown in this fig. 1 solid line is a second degree polynomial fit. Conclusion is consistent observation by L. Mahrt (2002) based on analysis of tower data from several SBL near surface quantities measured at 20 - 30 m above ground. μ is turbulence variable in the stable surface layer σ/U near to the surface and despite the fact the variance itself shows the greatest uncertainty near the surface. The composite value is 0.20 for study of night.

As shown in figure 3 distribution of the wind speed (top) show a greater wind resource potential for the layers of 45-200 m, and 45-250 m compare to the layer of 45-115 m currently occupied by turbine rotors. Standard deviation (middle) and turbulence intensity (bottom) also increase for the thicker layers and the shapes of distributions changed from (blue) normal to (red and green) skewed.

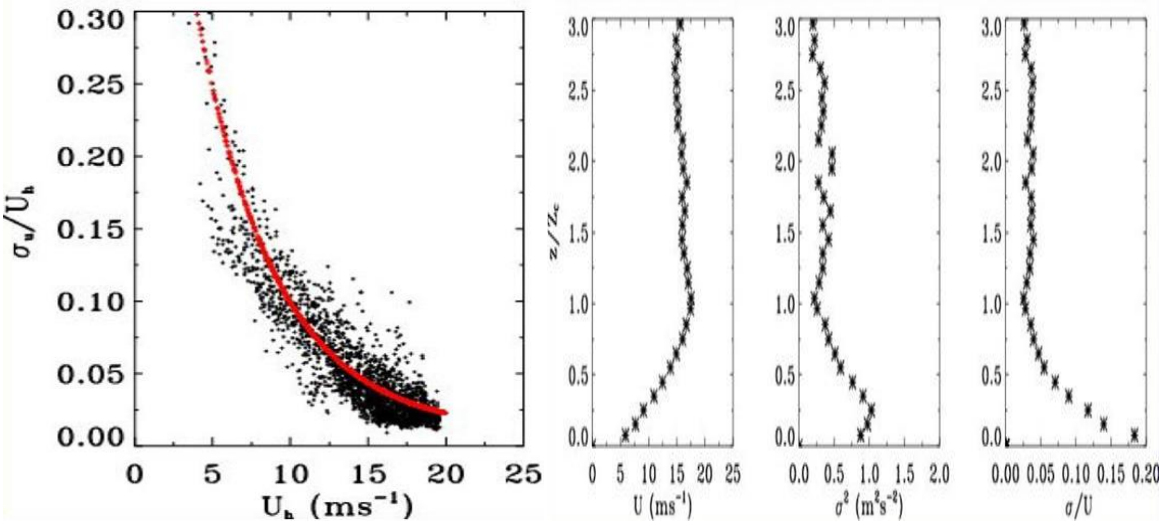

Fig. 1 Turbulence intensity, plotted against the horizontal wind speed for night and Fig. 2 Composite profile of U (ms^{-1}),$\sigma 2$ (m^{2}s^{-2}) turbulence and σ/U (Image courtesy: www.esrl.noaa.gov)

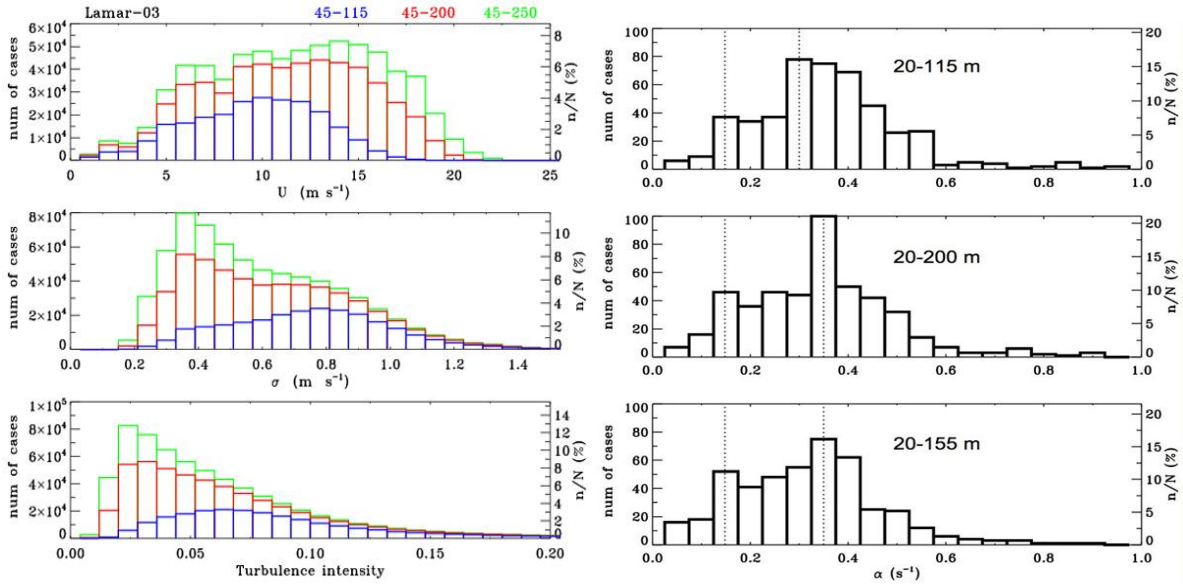

Fig. 3 Turbulence intensity and Fig. 4 Shear exponent by LIDAR at different height (Image courtesy: www.esrl.noaa.gov)

6.1 Wind shear across the rotor layer

Fig. 4 shown profiles of mean horizontal rate composited for every night of HRDL observations throughout LLJ, showing nearly linear wind shear up to 100-200 m. Its different color show the different time in UTC. In horizontally direction in this fig. 5 its shows the wind shear.

International Journal of Engineering Research & Technology (IJERT)
ISSN: 2278-0181
Vol. 7 Issue 02, February-2018

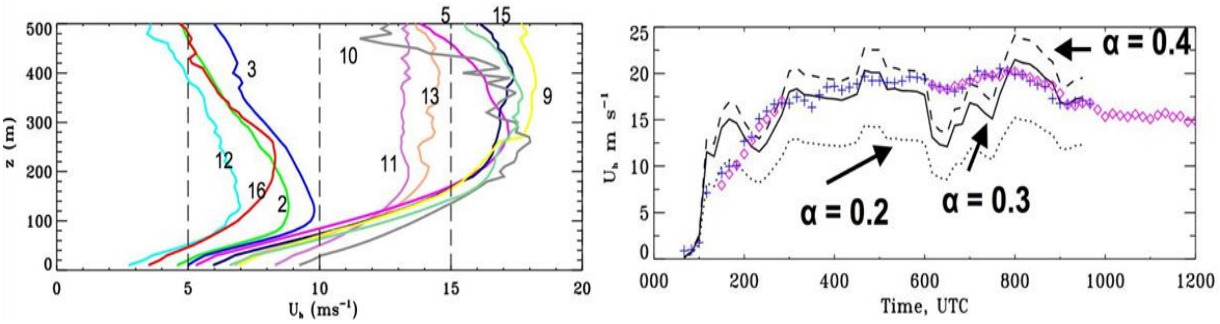

Fig. 5 Distribution of wind shear and Fig.6 Time series of LIDAR (Image courtesy: www.esrl.noaa.gov)

Distributions of the shear exponent (α) computed by lidar horizontal velocities measured at 115, 200, 250 and reference velocity at 20 m for the entire period of HRDL observations. In most cases α>0.20, with a dominant mode of 0.30-0.36.

7 DISUSSION:

Turbulence intensity as show in fig.1 gradually decreases (left to right), Turbulence Intensity may be a scale characterizing turbulence expressed as a percent. Associate degree perfect flow of air with fully no fluctuations in air speed or direction would have a Turbulence Intensity price of zero percentage. Now in fig.2 Composite profile of U (ms^{-1}),$\sigma 2$ (m^{2}s^{-2}) turbulence and σ/U we have to discussed there is three parametes on x axis which show fifferent parameter, U is show the jet speed, $\sigma 2$ turbulence compare to height, σ/U it show the turbulence intensity. Fig.2 first graph show it is increase and the constant up to 3 m, second one show the turbulence 0.8 m^{2}s^{-2} is gradually increase then suddenly decreases the constant at 1.0 z/z$_c$. Third shows the turbulence intensity similarly fig.1, as shows in fig.3 turbulence intensity show at different height. Distributions of the shear exponent (α) computed fig.4 by lidar horizontal velocities measured at 115, 200, 250 and reference velocity at 20 m for the entire period of HRDL observations. In most cases α > 0.20, with a dominant mode of 0.30-0.36. Fig.6 Time-series of the lidar (pluses) and high-confidence sodar (diamonds) wind speed measured at 200 m AGL and computed using the power law with a shear exponent of (solid) 0.30, (dashed) 0.40, and (dotted) 0.20 with a reverence wind speed measured by lidar at 20 m. LLJ wind profile shape, fig.5 as shows on may night time or afternoon time mixed layer accelerated uniformly with height after sunset to produce a nearly uniform profile of speed above z (m). Uniformly acceleration probably the as a result invariant geotropic winds and ageostrophic forcing with height. Fraction σ and TKE can be expressed of the speed of LLJ maximum, Ohya et al. (1997) equated with the streamline flow speed U, but measurement of U and σ are available for few studies. Verification structure only to extent that the atmosphere is both horizontally and stationary during the periods of ascent and descent generally on 10 min over distance of 10 km. Advantage and limitation of this technique are discussed by Mahrt (1985) and Tjernstrom and smedman (1993) Often TKE were not available down to near the surface, so profile may underestimate the maximum σ values. Estimates of U and σ from several studies, ratio of σ/U from individual profiles average range is 0.20. Consider a sampling technique appears to be impressive agreement with the result of our study. Another finding of this study was that the σ profile for the least stable cases tended to have traditional boundary layer structure with a maximum at the surface, stability increase slightly σ peak become evaluated. Another unsolved issue in the atmosphere which was addressed in the laboratory studies is the role of surface roughness. First study (Ohya et al. 1997) the wind tunnel lower boundary surface was smooth and second (Ohya 2001) the surface was roughened. In the first study peak values of σ^2 and σ/U which is approximately same in our study ~ 0.5 to 0.20. If results are transferable to the atmosphere we should expect only incremental increases in the σ/U ratio as a result roughness increases. Profile show by Nieuwstadt (1984), Lenschow et al. (1998) and Sorbjan (1988) show near value of turbulence at the SBL, profile measured by Smedman et al. (1993) and in wind tunnel show directly zero values of turbulence.

8. REFERENCES:

[1] Banta, R. M., Newsom, R. K., Lundquist, J. K., Pichugina, Y. L., Coulter, R. L., and Mahrt, L., 2002. Nocturnal low level jet characteristics over kansas during CASES-99. Bound. Layer Meteor. v. 105, pp 221-252.

[2] Banta, R. M., Pichugina, Y. L., and Newsom, R. K., 2003. Relationship between low level jet properties and turbulence kinetic energy in the nocturnal stable boundary layer. J. Atmos. Sci. v. 60, PP: 2549-2555.

[3] Banta R.M., Y.L. Pichugina, and W.A. Brewer, 2006. Turbulent Velocity-Variance Profiles in the Stable Boundary Layer Generated by a Nocturnal Low-Level Jet. J. Atmos. Sci., v. 62, PP: 2700-2719.

[4] Beyrich, F., 1994. Sodar observations of the stable boundary layer height in relation to the nocturnal low level jet. Meteor. Z., V. 3, PP: 29-34.

[5] Blackadar, A. K., 1957. Boundary layer wind maxima and their significance for the growth of nocturnal inversion. Bull. Amer. Meteor. Soc. v. 38, PP: 283-290.

[6] Cayghey, S. J., Wyngaard, J. C., Kaimal, J. C., 1979. Turbulence in the evolving stable boundary layer, J. Atmos. Sci. v. 36, PP: 1041-1052.

[7] Drobinski, P. P., Carlotti, R. K., Newsom, R., Banta, M., Foster, R. C., and Redelsperger, J. L., 2004. The Structure of the nearneutral atmospheric surface layer. J. Atmos. Sci., v. 61, pp 699-714.

[8] Grund, C. J., Banta, R. M., George, J. L., Howell, J. N., Post, M. J., Richter, R. A., and Weickmann, A. M., 2001. High resolution Dopplar lidar for boundary layer and cloud research. J. Atmos. Oceanic Technol. v. 18, PP: 376-393.

International Journal of Engineering Research & Technology (IJERT)
ISSN: 2278-0181
Vol. 7 Issue 02, February-2018

[9] Hogstrom, U., and Smedman, 1984. The wind regime in coastal area with special reference to result from the swedish wind energy program, Bound layer Meteor. v. 30, PP: 351-373.
[10] Kelley, N. D., Shirazi, M., Jager, S., Wilde, S., Admas, J., Buhl, M., Sullivan, P., and Patton, E., 2004. Lamar low level jet project interim report, Tech. Rep. NREL/TP-500-34593, national renewable energy laboratory, Golden, CO, PP: 182.
[11] Kosovic, B., and Curry, J., 2000. A large eddy simulation study of a quasi steady stable stratified atmospheric boundary layer, J. Atmos. Sci. v. 57, PP: 1052-1068.
[12] Lehschow, D. H., Li, X. S., Zhu, C. J., and Stankov, B. B., 1988. The stably stratified boundary layer over the great plains, I mean and turbulent structure. Bound. Layer Meteor., v. 42, PP: 95-121.
[13] Mahrt, L., Heald, R. C. Heald, Lenchow, D. H., Stankov, B. B., and Troen, I., 1979. An observational study of the structure of the nocturnal boundary layer, Bound. Layer Meteor. v. 17, PP: 247-264.
[14] Mahrt, L., 1985. Vertical structure and turbulence in the very stableboundary layer. J. Atmos. Sci., v. 42, PP: 2333-2349.
[15] Mahrt, L., and Vickers, D., 2002. Contrasting vertical structure of nocturnal boundary layers, Bound. Layer Meteor. v. 105, PP: 351-363.
[16] Nieuwstadt, F. T. M., 1984. The turbulent structure of the stable nocturnal boundary layer, J. Atmos. Sci. v. 41, PP: 2202-2216.
[17] Ohya. Y., D. E. Neff, and Meroney, R. N. 1997. Turbulence structure in a straisfied boundary layer under stable conditions. Bound. Layer Meteor., v. 83, PP: 139-161.
[18] Ohya, Y., 2001. Wind tunnel study of atmospheric stable boundary layers over a rough surface. Bound. Layer Meteor., v. 98, PP: 57-82.
[19] Poulos, G. and Coauthors 2002. CASES-99, A comprensive ivestigation of the stable nocturnal boundary layer, Bull. Amer. Meteor. Soc. v. 83, PP: 551-581.
[20] Saiki, E. M., Moeng, C. H., and Sullivan, P. P., 2000. Large eddy simulation of a stably stratified planetray boundary layer. Bound. Layer Meteor. v. 95, PP: 1-30.
[21] Smedman, A. S., Tjernstrom, M., and Hogstrom, U., 1993. Observations of a multi level turbulence structure in a very stable atmospheric boundary layer. Bound. Layer Meteor., v. 44, PP: 231-253.
[22] Smedman, A. S., Tjernstrom, M., and Hogstrom, U., 1995. Spectra variances and length scales in a marine stable boundary layer deminated by a low level jet. Bound. Layer Meteor., v. 76, PP: 221-232.
[23] Smedman, A. and Grisogono, B., 1997. Evolution of stable internal boundary layer over a cold sea. Geophys. Res., v. 102, PP: 1091-1099.
[24] Smedman, A., Hogstrom, U., and Hunt, J. C. R., 2004. Effect of shear sheltering in a stable atmospheric boundary layer with strong shear. Quart J. Roy. Meteor. Soc. V. 103, PP: 31-50.
[25] Sorbjan,Z., 1988. Structure of the stably stratified boundary layer during the SESAME-1979 expariment. Bound. Layer Meteor. v. 44, PP: 255-266.
[26] Tjernstrom, M., and Smedman, A. S., 1993. The vertical turbulence structure of the coastal marine atmospheric boundary layer. J. Geophys. Res., v. 98, PP: 4809-4826.
[27] Wulfmeyer, V. O., Randall, M., Brewer, W. A., and Hardesty, R. M., 2000. 2 µm Doppler lidar transmitter with high free squency stability and low chirp, Opt. Lett. V. 25, PP: 1228-1230.